JMEPEG (2012) 21:180–190
DOI: 10.1007/s11665-011-9963-7

1059-9495/$19.00

A Numerical Method for Inverse Thermal Analysis of Steady-State Energy Deposition in Plate Structures

S.G. Lambrakos, A.D. Zervaki, and G.N. Haidemenopoulos

(Submitted March 23, 2011)

A numerical method for inverse thermal analysis of steady-state energy deposition in plate structures is constructed according to the general physical characteristics of energy deposition within a volume of material from a beam energy source. This numerical method represents implementation of a general methodology using basis functions that was introduced previously. The formal structure of the numerical method presented follows from a specific definition of the inverse heat transfer problem, which is well posed for inverse analysis of heat deposition processes. This definition is based on the assumption of the availability of information concerning spatially distributed boundary and constraint values. This information would be obtained in principle from both experimental measurements obtained in the laboratory, as well as numerical simulations performed using models having been constructed using basic theory. Experimental measurements include solidification cross sections, thermocouple measurements, and microstructural changes.

Keywords aluminum, modeling processes, welding

1. Introduction

In what follows a numerical method for inverse analysis of energy deposition processes is constructed according to the general physical characteristics of energy deposition within a volume of material from a beam energy source. This numerical method represents an implementation of a general methodology using basis functions that was introduced previously. The formal structure of the numerical method presented follows from a specific definition of the inverse heat transfer problem, which is well posed for inverse analysis of heat deposition processes. This definition is based on the assumption of the availability of information concerning spatially distributed boundary and constraint values. This information would be obtained in principle from both experimental measurements obtained in the laboratory, as well as numerical simulations performed using models having been constructed using basic theory. Experimental measurements include solidification cross sections, thermocouple measurements, and microstructural changes. Numerical simulation data include general temperature field trend characteristics, response characteristics of materials to volumetric energy deposition, and the relative sensitivity of temperature field characteristics to phenomena occurring on different space and time scales.

The construction of temperature fields according to spatially and temporally distributed constraint conditions using linear combinations of optimal basis functions represents a highly convenient approach to inverse analysis of energy deposition processes. This approach can be extended, however, using a numerical methodology that provides even more flexibility for the construction of temperature fields according to constraint conditions. This numerical methodology employs linear combinations of optimal basis functions for the purpose of assigning boundary condition values and initial estimates of the temperature field, which are for subsequent adjustment according to constraint conditions. Basis functions can be terms of either analytic or numerical function representations, or both in linear combination. Analytic function representations are fundamental solutions to the heat conduction equation for relatively simple workpiece geometries, e.g., plate structures having a finite thickness. Numerical function representations are linear combinations of temperature histories that have been tabulated and stored as discrete functions.

The organization of the subject areas presented here is as follows. First, a precise mathematical statement is given of the inverse problem for which the numerical method is constructed. In that the range of inverse problems is vast, it is essential to define precisely the inverse problem to be addressed. This definition represents a generalization of similar, but more restrictive, definitions given previously (Ref 1-4). Second, a general formulation of the numerical method for inverse analysis of steady-state heat deposition within plate structures is presented. Third, a discussion is given that concerns various mathematical aspects of the numerical method presented. This discussion emphasizes that many aspects of the numerical method can be further developed with respect to both algorithmic structure and implementation. Fourth, a prototype analysis is presented for the purpose of providing an illustrative example of some specific aspects of the numerical method. In particular, that the numerical method can provide weld temperature histories that can be adopted as input data to various types of computational procedures, such as those for prediction of solid state phase transformations and their associated software implementations. And in addition, that weld temperature histories calculated using this method can be

S.G. Lambrakos, Materials Science and Technology Division, Center for Computational Materials, Naval Research Laboratory, Code 6390, Washington, DC; and **A.D. Zervaki** and **G.N. Haidemenopoulos**, Department of Mechanical Engineering, University of Thessaly, 38334 Volos, Greece. Contact e-mail: lambrakos@anvil.nrl.navy.mil.

used to construct numerical basis functions, which can be adopted for inverse analysis of welds corresponding to other process parameters or of welding processes whose process conditions are within similar regimes. Finally, a conclusion is given.

2. Definition of Inverse Heat Deposition Problem

The inverse heat transfer problem (Ref 1-4) may be stated formally in terms of source functions (or input quantities) and multidimensional fields (output quantities). The statement of the inverse problem given here is focused on aspects of inverse heat deposition problem related to the determination of heat fluxes via appropriate regularization of their spatial and time distributions. This statement represents an extension of that given in Ref 5. In general, the formulation of a heat conductive system occupying an open bounded domain Ω with an outer boundary S_o and an inner boundary S_i involves the parabolic equation

$$\frac{\partial T(\hat{x},t)}{\partial t} + \hat{V}(\hat{x},t)\cdot\nabla T(\hat{x},t) = \nabla\cdot(\kappa(\hat{x},t)\nabla T(\hat{x},t)) + Q(\hat{x},t) \quad \text{(Eq 1a)}$$

for $T(\hat{x},t)$ in $\Omega\times(0,t_f)$, with initial condition $T(\hat{x},0) = T_a(\hat{x})$ in Ω, and Dirichlet boundary conditions on the inner and outer boundaries, S_i and S_o, respectively, as follows:

$$T(\hat{x},t) = T_i(\hat{x}_s,t) \quad \hat{x}_s \in S_i \quad \text{(Eq 1b)}$$

on $S_i\times(0,t_f)$, and

$$T(\hat{x},t) = T_o(\hat{x}_s,t) \quad \hat{x}_s \in S_o \quad \text{(Eq 1c)}$$

on $S_o\times(0,t_f)$. Here $\hat{x} = (x,y,z)$ is the position vector, t_f is the final time, $T(\hat{x},t)$ is the temperature field variable, $\kappa(\hat{x},t)$ is the thermal diffusivity field variable, $T_a(\hat{x})$, $T_i(\hat{x},t)$, and $T_o(\hat{x},t)$ are specified functions, and $Q(\hat{x},t)$ is the volumetric heat source function. Determination of the temperature field via solution of Eq 1a to 1c defines the direct initial-boundary value problem. The inverse problem considered here is that of reconstructing the temperature field $T(\hat{x},t)$ for all time $t\in[0,t_f]$ based on available information concerning the functions defined by Eq 1b and 1c. This information must be acquired either experimentally or via direct numerical simulation.

Following the inverse analysis approach, a parametric representation based on a physical model provides a means for the inclusion of information concerning the physical characteristics of a given energy deposition process. It then follows that for heat deposition processes involving the deposition of heat within a bounded region of finite volume, consistent parametric representations of the temperature field are given by

$$T(\hat{x},t) = T_A + \sum_{k=1}^{N_k} w_k T_k(\hat{x},\hat{x}_k,\kappa,t) \quad \text{and} \quad T(\hat{x}_n^c,t_n^c) = T_n^c \quad \text{(Eq 2)}$$

where $T_k(\hat{x},\hat{x}_k,\kappa,t)$ represent an effectively complete set of basis functions for representation of the temperature field within the region bounded by surfaces S_i and S_o. The quantity T_A is the ambient temperature of the workpiece and the locations $\hat{x}_n^c$ and temperature values T_n^c specify constraint conditions on the temperature field. The functions $T_k(\hat{x},\hat{x}_k,\kappa,t)$ represent an optimal, or effectively complete, basis set of functions for given boundary conditions and material properties. The quantities $\hat{x}_k = (x_k,y_k,z_k)$, $k = 1,\ldots,N_k$, are the locations of the elemental source or boundary elements. Selection of an optimal set of basis functions is based on a consideration of the characteristic model and data spaces of heat deposition processes and subsequently isolating those regions of the model space corresponding to parameterizations that are both physically consistent and sufficiently general in terms of their mathematical representation and mapping from data to model space (Ref 6). Although heat deposition processes may be characterized by complex coupling between the heat source and the workpiece, as well as complex geometries associated with either the workpiece or the deposition process, in terms of inverse analysis the general functional forms of the temperature fields associated with all such processes are within a restricted class of functions, i.e., optimal sets of functions. Accordingly, a sufficiently optimal set of functions are the analytic solutions to heat conduction equation for a finite set of boundary conditions (Ref 7). A parameterization based on this set is both sufficiently general and convenient relative to optimization.

The formal procedure underlying the inverse method considered here entails the adjustment of the temperature field defined over the entire spatial region of the sample volume at a given time t. This approach defines an optimization procedure where the temperature field spanning the spatial region of the sample volume is adopted as the quantity to be optimized. Constraint conditions are imposed on the temperature field spanning the bounded spatial domain of the workpiece by minimization of the objective function defined by

$$Z_T = \sum_{n=1}^{N} w_n\left(T(\hat{x}_n^c,t_n^c) - T_n^c\right)^2, \quad \text{(Eq 3)}$$

where T_n^c is the target temperature for position $\hat{x}_n^c = (x_n^c,y_n^c,z_n^c)$. The input of information into the inverse model defined by Eq 1 to 3, i.e., the mapping from data to model space, is effected by: the assignment of individual constraint values to the quantities T_n^c; the form of the basis functions adopted for parametric representation; and specifying the shapes of the inner and outer boundaries, S_i and S_o, respectively, which bound the temperature field within a specified region of the workpiece. The constraint conditions and basis functions, i.e., $T(\hat{x}_n^c,t_n^c) = T_n^c$ and $T_k(\hat{x},\hat{x}_k,\kappa,t)$, respectively, provide for the inclusion of information that can be obtained from both laboratory and numerical experiments (Fig. 1).

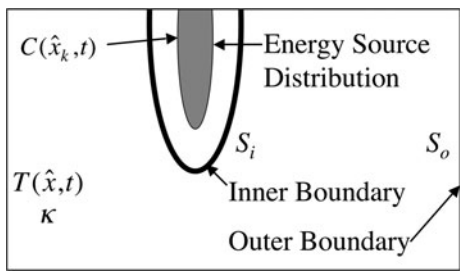

Fig. 1 Schematic representation of inner and outer boundaries of temperature field that define inverse steady-state heat deposition problem

The existence of a convenient and general parameterization of inner boundary surfaces, $T(\hat{x}_s)$, $\hat{x}_s \in S_i$, bounding the temperature fields associated with heat deposition processes is conjectured based on the obvious fact that all heat deposition processes are characterized by thermal and energy deposition profiles whose general form can be represented by a small class of geometric shapes. This conjecture is plausible and is based on the fact that the observed volumetric distributions of energy from all types of heat deposition processes, within the inner boundary S_i of their associated temperature fields, can be represented by linear combinations of the basis functions having the form of a modified Beer Lambert Law. These arguments establish a plausible foundation for the existence of a relatively optimal and general parametric representation $T(\hat{x}, \kappa, V, l, T_b(\hat{x}_s), \hat{x}_s \in S_i, S_o)$ for inverse analysis of heat deposition processes. In doing so, referring to Fig. 2, the inverse problem defined by the mapping

$$C(\hat{x}_k, t), \kappa \mapsto T(\hat{x}, t) \qquad \text{(Eq 4a)}$$

is replaced by the inverse problem defined by the mapping

$$C(\hat{x}_k, t), \kappa \mapsto S_i, S_o \mapsto T(\hat{x}, t) \qquad \text{(Eq 4b)}$$

The inverse problem as defined by Eq 4b can be extended to include systems that are characterized by incomplete information concerning the diffusivity κ, as well as any nonlinear dependence of κ on temperature. This follows in that the inverse problem defined by Eq 4b adopts the quantities $C(\hat{x}_k, t)$ and κ as surface generators. Accordingly, the mapping defined by Eq 4b can be generalized to include discrete distributions of diffusivities, i.e.,

$$C(\hat{x}_k, t), \kappa_k \mapsto S_i, S_o \mapsto T(\hat{x}, t) \qquad \text{(Eq 4c)}$$

Given an inverse analysis formulation that is defined by the sequence of mappings Eq 4c, relatively interesting sensitivity issues are observed to follow. The mathematical properties underlying these sensitivity issues are the same as those responsible for the ill posedness of many inverse analysis procedures based on the mapping Eq 4a. That is to say, those filter properties of diffusion processes that tend to make the temperature field $T(\hat{x}, t)$ insensitive to details of the shape of the source distribution $C(\hat{x}_k, t)$, tend to make $T(\hat{x}, t)$ insensitive to details of the shapes of S_i and S_o. This insensitivity to details of the shapes of S_i and S_o, e.g., the shape of the solidification boundary, implies that a general parametric representation of the inner and outer boundaries can in principle be formulated in terms of a reasonably convenient mathematical form. For these analyses the heat source distribution assumes the role of a boundary surface generator. This interpretation of $C(\hat{x}_k, t)$ permits convenient parameterization of S_i and S_o.

3. Numerical Methodology

Presented in this section is a numerical method for inverse analysis of heat deposition processes. With respect to the

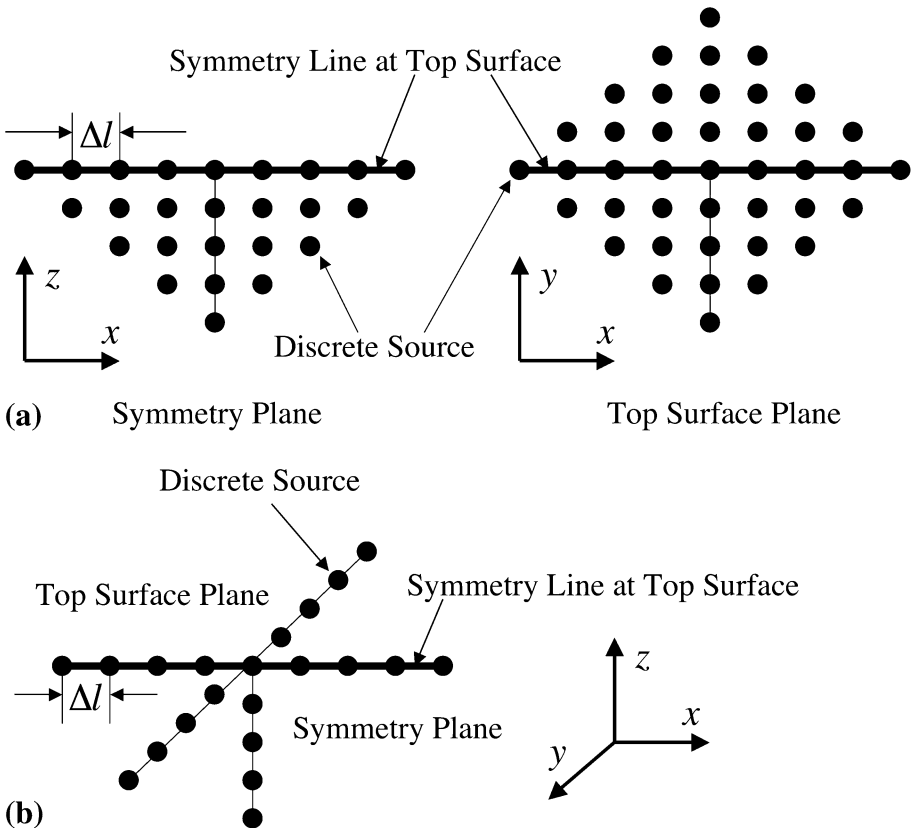

Fig. 2 (a) General form of discrete distribution of energy sources for generation of inner boundary S_i and corresponding temperature field. (b) Conveniently adjustable form of discrete distribution of energy sources for generation of inner boundary S_i and corresponding temperature field

numerical method presented, a set of basis functions is considered effectively complete if these functions provide reasonably optimal fitting to boundary and constraint conditions. Before proceeding it is significant to note that in principle the set of basis functions adopted by Eq 2 can be defined in terms of either analytical or numerical function representations. The numerical method that is developed here employs both analytical and numerical function representations of basis function adopted for the calculation of temperature fields within bounded domains within which constraint conditions are specified. In addition, the interrelation between analytical and numerical basis function representations is an important aspect of the numerical method. Proceeding, a consistent representation Eq 2 of the temperature field for heat deposition within structures characterized by a finite thickness, in terms of analytical basis functions, is given by

$$T(\hat{x},t) = T_{\mathrm{A}} + \sum_{k=1}^{N_k}\sum_{n=1}^{N_t} C(\hat{x}_k)G(\hat{x},\hat{x}_k,\kappa,V,n\Delta t) \qquad \text{(Eq 5)}$$

where

$$G(\hat{x},\hat{x}_k,\kappa,V,t) = \frac{1}{t}\exp\left[-\frac{(x-x_k-Vt)^2+(y-y_k)^2}{4\kappa t}\right] \times\left\{1+2\sum_{m=1}^{\infty}\exp\left[-\frac{\kappa m^2\pi^2 t}{l^2}\right]\cos\left[\frac{m\pi z}{l}\right]\cos\left[\frac{m\pi z_k}{l}\right]\right\} \qquad \text{(Eq 6)}$$

and

$$C(\hat{x}) = \sum_{k=1}^{N_k} Q(\hat{x}_k)\delta(\hat{x}-\hat{x}_k) \qquad \text{(Eq 7)}$$

The quantities κ, V, and l are the thermal diffusivity, welding speed, and plate thickness, respectively. Referring to Eq 7, it is significant to note that with respect to numerical methods, all analytical representations of the energy source function are in fact a precursor to some type of discrete representation for subsequent numerical implementation. The procedure for inverse analysis defined by Eq 5 to 7 entails adjustment of the parameters $C(\hat{x}_k)$, $\hat{x}_k$, and Δt defined over the entire spatial region of the workpiece. Shown in Fig. 2 is schematic representations of the discrete source distributions corresponding to the parameterizations defined by Eq 7.

Next, it should be noted that the linear combination of basis functions defined by Eq 5 can be extended to include an implicit specification of an average diffusivity field $\langle\kappa(\hat{x})\rangle$, which is consistent with the sequence of mappings defined by Eq 4c. This linear combination is of the form

$$T(\hat{x},t) = T_{\mathrm{A}} + \sum_{k=1}^{N_k}\sum_{n=1}^{N_t} C(\hat{x}_k,\kappa_k)G(\hat{x},\hat{x}_k,\kappa_k,n\Delta t) \qquad \text{(Eq 8)}$$

Having generated temperature histories at discrete transverse locations (y_m, z_m), a consistent representation given by Eq 2 of the temperature field for heat deposition within structures characterized by a finite thickness, in terms of numerical basis functions, is given by

$$T(\hat{x},t) = T_{\mathrm{A}} + \sum_{m=1}^{N_m} A_m T_m(\hat{x},y_m,z_m,\kappa,l,V,S_{\mathrm{i}},S_{\mathrm{o}}) \qquad \text{(Eq 9)}$$

where (y_m, z_m) are discrete transverse locations at which steady-state temperature histories have been tabulated and thus provide a numerical basis function representation.

4. Construction of A Parametric Field Representation for Steady-State Energy Deposition

The set of basis functions presented above provide a general parametric representation for inverse analysis of welding processes. Given these basis functions, the temperature field associated with any given process for steady-state energy deposition within plate structures is completely specified by a given set of inner and outer bounding surfaces S_{i} and S_{o}, respectively, the temperature distributions over these surfaces, a specified average diffusivity, κ, speed of deposition, V, and the thickness, l, of the workpiece. Accordingly, it follows that one is able to define a multidimensional temperature field $T(\hat{x},t,\kappa,V,l,T_s(\hat{x}_s),\ \hat{x}_s \in S_{\mathrm{i}},S_{\mathrm{o}})$. It is significant to note, however, that this multidimensional field provides a parametric representation, i.e., parameterization, of welding processes to the extent that any of the different possible types of boundary surfaces S_{i} and S_{o}, associated with these processes can be represented conveniently and an average κ can be specified. This is certainly the case since the volumetric source function $C(\hat{x}_k)$ assumes the role of a boundary surface generator, and therefore provides a framework for parameterization of S_{i} and S_{o} using the basis functions given above.

A general procedure for construction of a multidimensional temperature field $T(\hat{x},t,\kappa,V,l,T_s(\hat{x}_s),\ \hat{x}_s \in S_{\mathrm{i}},S_{\mathrm{o}})$ can now be described using the illustrative example that follows. The basis of this procedure is that for welding processes associated with a given class of materials, e.g., metals, the range of different possible shapes of inner boundary surfaces S_{i} is denumerably finite and that diffusivities and workpiece dimensions are bounded within a reasonable range of values. Accordingly, a general procedure for construction of $T(\hat{x},t,\kappa,V,l,T_s(\hat{x}_s),\ \hat{x}_s \in S_{\mathrm{i}},S_{\mathrm{o}})$., which can be interpreted as evolutionary, is based on the systematic accumulation of results of inverse analyses applied to various types of experimental measurements and numerical simulations. This procedure can be described with reference to Fig. 3 and 4 which describes its relationship to the calculation of temperature fields for welding processes using inverse analysis in general. Referring to this figure, it is to be further noted that the results of various inverse analyses, which involve different types of deposition processes can be stored. In addition, as in the illustrative example that follows, for a given inverse analysis where S_{i} has been specified, one can vary κ and l over their entire range of possible values and then store the associated temperature fields. A natural consequence of the finite range of shapes of S_{i} and of values of κ and l is that the stored temperature fields can evolve into a discrete multidimensional temperature field that is sufficiently dense for interpolation between field values. Again referring to Fig. 3, it can be noted that a discrete multidimensional temperature field, having been constructed and sufficiently dense, can be used for objective function minimization as an alternative to parametric

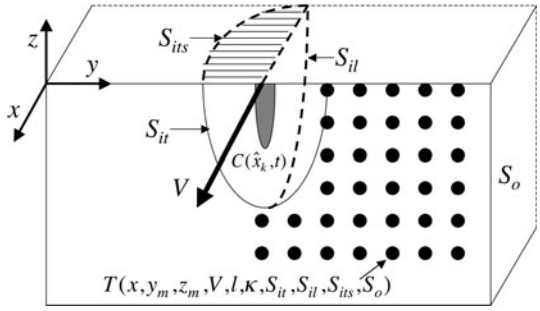

Fig. 3 Temperature field parameterization with respect to experimentally observable solidification boundaries for construction of numerical basis functions

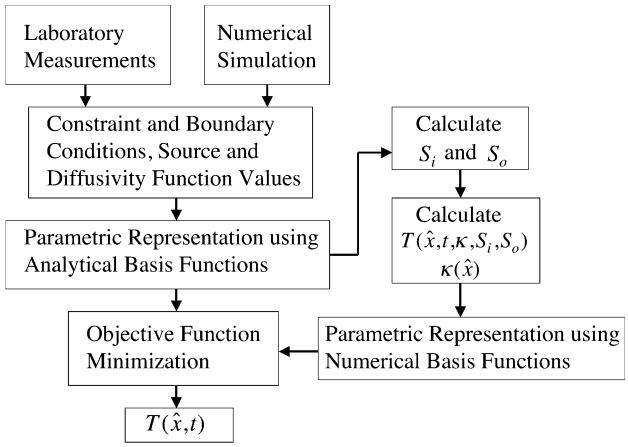

Fig. 4 General procedure for calculation of temperature fields for energy deposition processes using inverse analysis

representation using "analytical" basis functions. It follows that an alternative parameterization to that using the basis functions defined by Eq 6 to 9 is given by

$$T(\hat{x},t) = T_A + \sum_{m=1}^{N_m} A_m T_m(\hat{x}, y_m, z_m, \kappa, l, V, S_{it}, S_{il}, S_{its}, S_o) \quad \text{and}$$
$$T(\hat{x}_n^c, t_n^c, \kappa) = T_n^c \qquad \text{(Eq 10)}$$

where A_i, $i = 1, \ldots, N_i$, are weight coefficients for effecting interpolation within the multidimensional space define by $(\hat{x}, t, \kappa, V, l, S_{it}, S_{il}, S_{its})$. As with the basis functions defined by Eq 8 and 9, which are based on a generalized function representation, the functions $T(\hat{x}, t, \kappa, V, l, S_{it}, S_{il}, S_{its})$ provide for the specification of a numerical basis function representation of the temperature field.

According to the procedure defined by Fig. 3 and 4, the basis function expansions given by Eq 6 and 10 can be interpreted as two equivalent parametric representations, each of which is associated with four parameters. In the case of Eq 6, which is in terms of analytic basis functions, these parameters are $C(\hat{x}_k, t)$, $\hat{x}_k$, t_k and diffusivity. In the case of Eq 10, which is in terms of numerical basis functions, these parameters are the welding speed, thickness of workpiece, shape of inner boundary S_i and diffusivity. Given in the next section is an example of a general procedure, which follows from the equivalence of Eq 6 and 10, for construction of a parametric temperature field in terms of numerical basis functions.

It is significant to note that the constraint conditions defined by the three cross section surfaces S_1, S_2, and S_3 provide sufficient bounding of the calculated temperature field to the extent that the entire three-dimensional shape of the of the solidification boundary is constrained to be within a reasonable approximation. That is to say, although the calculated three-dimensional shape of the solidification boundary is not in principle unique, its range of variability is expected to be so very limited that it is essentially unique for all practical purposes.

5. Construction of Numerical Basis Functions

The general procedure for construction of numerical basis functions entails calculation of the steady-state temperature field for a specified range of sizes and shapes of the inner surface boundary S_i for a given welding, or in general, heat deposition process. In the case of welding processes, rather than constructing a temperature field that is a function of a closed surface S_i, a more realistic construction should consider temperature field dependence on the experimentally observable solidification boundaries S_{it}, S_{il}, and S_{its} that are shown in Fig. 3. Accordingly, the example of a multidimensional temperature field construction presented here adopts the laser beam welds, whose cross sections are shown in Fig. 5 to 7 as three different sets of values for S_{it}, S_{il}, and S_{its} that are relatively close to each other in parameter space. It is significant to note that for the present analysis the exact focal points of the electron beams for the welds are not relevant. The goal of the present analysis is simply to adopt a set of process parameters that produce sets of values for S_{it}, S_{il}, and S_{its} that are relatively close. For this system, the parameter values assumed are $\kappa = 1.88 \times 10^{-5} \cdot m^2/s$, $T_M = 567$ °C (solidus temperature of 2198-T8 Aluminum) $l = 3.8$ mm and $V = 3.33$ cm/s. The upstream boundary constraints on the temperature field, $T_c = T_M$ for (y_c, z_c) defined in Eq 2, are given in Table 1. Shown in Fig. 8 to 10 are different planar slices of the time-dependent temperature field that have been calculated according to the constraint conditions given in Table 1 for energy surface deposition of 103 J/mm.

The general procedure for constructing a multidimensional temperature field for a given welding process follows with reference to Fig. 5 to 7. Accordingly, these temperature histories represent two hypersurfaces that are close to each other in the parameter space for $T(\hat{x}, t, \kappa, V, l, S_{it}, S_{il}, S_{its})$. Construction of a multidimensional temperature field is effected by adjustment of process parameters such that S_{it}, S_{il}, and S_{its} span a range of values that include all process conditions. For each set of values of S_{it}, S_{il}, and S_{its}, temperature histories $T(\hat{x}, t, \kappa, V, l, S_{it}, S_{il}, S_{its})$ are calculated for specified values of κ, V, and l. This procedure is then followed for incremental changes of the parameters κ, V, and l.

6. Discussion

It is important to note that Eq 3 to 6 can be interpreted from the view point of numerical methods, rather than that of a discrete approximate representation of an analytical solution to the heat conduction equation. With respect to this

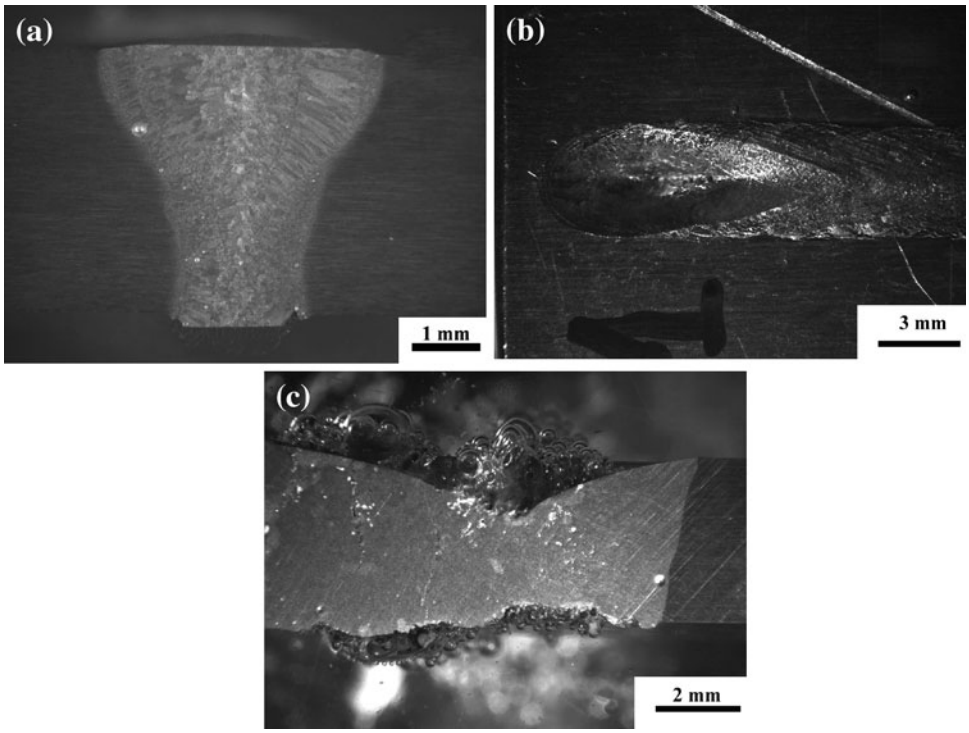

Fig. 5 Laser beam weld of Al 2198-T8 for energy deposition of 103 J/mm and beam focal point at 1 mm above top surface of workpiece. (a) Transverse cross section. (b) Top surface of workpiece. (c) Longitudinal cross section at symmetry plane. Beam power and welding speed are 3441 W and 2 m/min, respectively

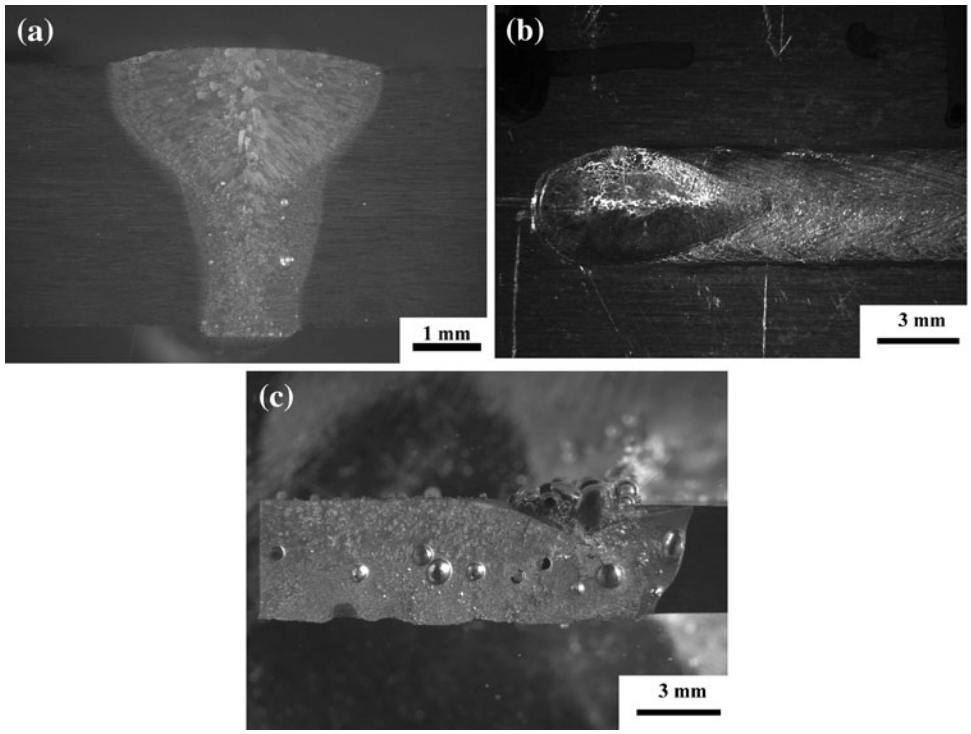

Fig. 6 Laser beam weld of Al 2198-T8 for energy deposition of 103 J/mm and beam focal point at 1 mm below top surface of workpiece. (a) Transverse cross section. (b) Top surface of workpiece. (c) Longitudinal cross section at symmetry plane. Beam power and welding speed are 3441 W and 2 m/min, respectively

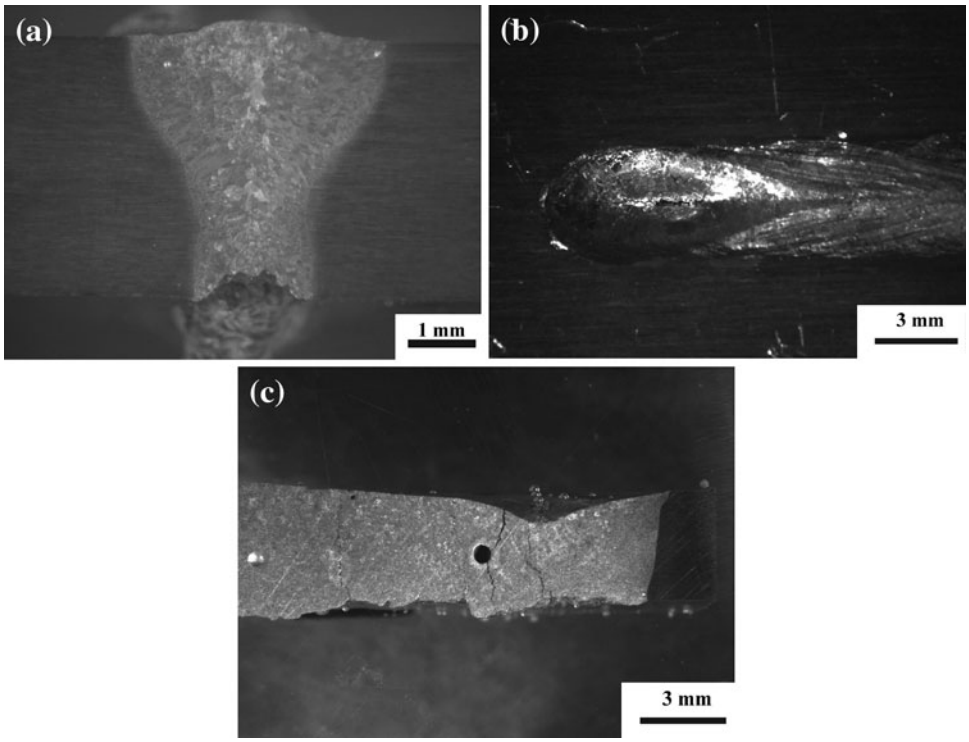

Fig. 7 Laser beam weld of Al 2198-T8 for energy deposition of 103 J/mm and beam focal point at top surface of workpiece. (a) Transverse cross section. (b) Top surface of workpiece. (c) Longitudinal cross section at symmetry plane. Beam power and welding speed are 3441 W and 2 m/min, respectively

Table 1 Temperature field constraint conditions at positions (y_c, z_c) on transverse cross sections of welds at solidification boundaries

Focal point z_c, mm	1 mm $2y_c$, mm	−1 mm $2y_c$, mm	0 mm $2y_c$, mm
0.0	4.25	4.0	4.375
0.5	3.875	3.875	4.25
1.0	3.25	3.5	3.75
1.5	2.125	2.75	2.75
2.0	1.875	2.175	2.375
2.5	1.625	1.875	2.125
3.0	1.5	1.75	1.875
3.5			2.0
3.8	1.5	1.875	2.125
Figure	5	6	7

interpretation, Eq 3 to 6, given the condition defined by Eq 6, represents a discrete form of Eq 9 that is unconditionally stable with respect to timestep size.

The starting point for the construction of a numerical method for calculating time-dependent temperature histories for any given energy deposition process is a discrete representation of the heat conduction equation. In terms of finite differences, discrete representations of this equation, for calculation of time-dependent temperature fields, fall within two classes, explicit or implicit schemes (see Ref 8 for further discussion). These classes are defined according to numerical stability conditions, which determine the nature of error propagation as a function of time. Explicit schemes are characterized by relatively strict stability conditions on the choice of discrete timestep size. Implicit schemes are characterized by unconditional stability with respect to timestep size. With respect to explicit schemes, owing to a well-defined criterion for numerical stability, there exist an a priori measure, or rather sense, of error propagation within the calculated temperature fields as a function of time. This a priori measure of accuracy for calculated temperature fields comes at the very high price of very small timestep sizes, which renders many heat transfer problems intractable with respect to numerical simulation via explicit schemes. Implicit schemes, owing to their unconditional stability with respect to timestep size, are well posed for numerical simulations of heat transfer over time and space scales that are of practical significance relative to process modeling. In general, however, it is difficult to access the accuracy of these schemes in that there does not exist rigorous criteria for error propagation. Typically, implicit schemes for discrete representation of the heat conduction equation are structured in terms of linear-algebraic formulations. These formulations provide a framework for the construction of various types of algorithms for purposes of numerical simulation.

It follows that, in terms of the classification of discrete representations of the heat conduction equation, the parametric representations Eq 3 to 5, which are constructed using linear combinations of analytical basis functions, provide an unconditionally stable method for calculation of time-dependent temperature fields. With the understanding that Eq 1 to 5 represents an unconditionally stable method for calculation of temperature histories, the problem of establishing some assessment of error propagation as a function of time becomes of relevance.

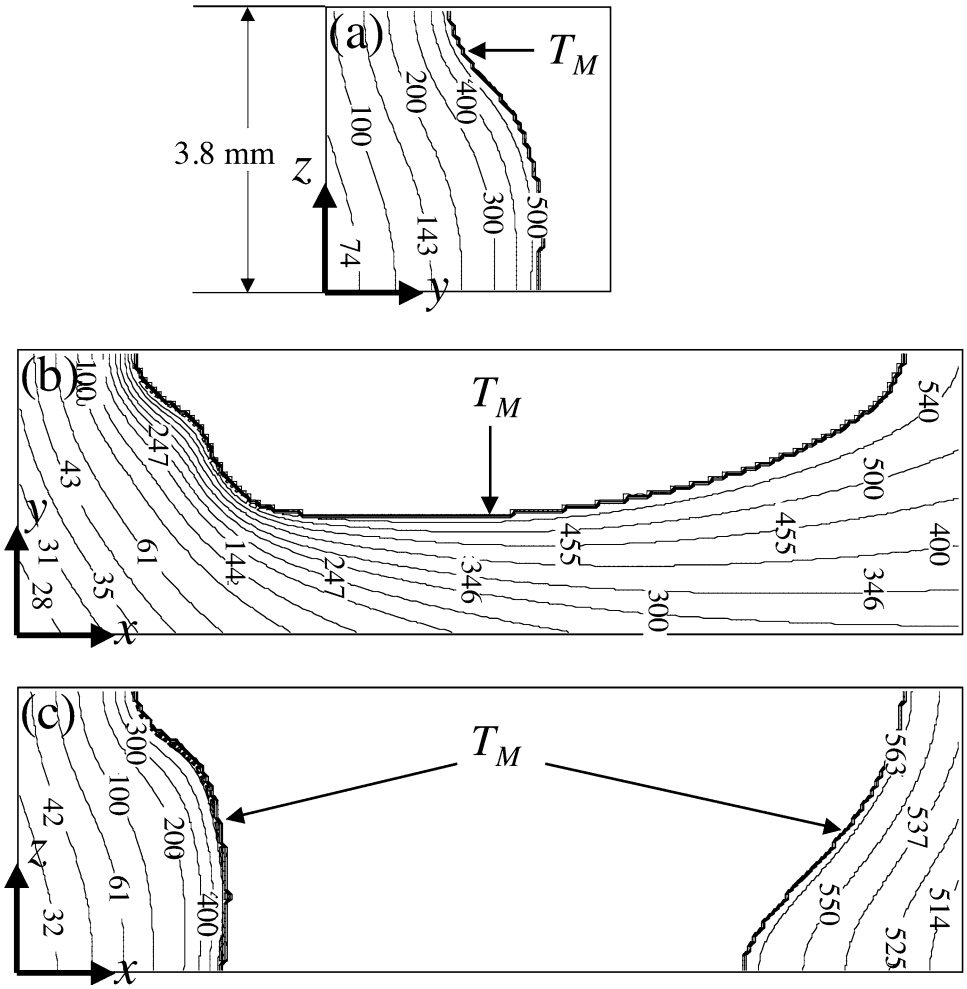

Fig. 8 Two-dimensional slices of three-dimensional temperature field (°C) calculated using cross section information shown in Fig. 5. (a) Transverse cross section. (b) Top surface of workpiece. (c) Longitudinal cross section at symmetry plane

At this stage, it is important to indicate that the classifications explicit and implicit, for discrete representations of the heat conduction equation, are motivated primarily by a direct-problem perspective for numerical modeling of physical processes. With respect to this perspective, the discrete representation Eq 3 to 5 can be applied for qualitative analysis of physical characteristics of a given energy deposition process. This follows in that the calculated temperature field, although possibly not quantitatively accurate for relatively large time steps, is able to "shadow" the actual field to the extent that all qualitative trend features are preserved. This is a general characteristic of many implicit schemes. Accordingly, selection of an appropriate timestep size for qualitative accuracy can be verified by examination of the extent to which a calculated solution can shadow a physical consistent solution.

In principle, with respect to an inverse-problem perspective for numerical modeling of energy deposition processes, the discrete representation Eq 2 to 5 can be applied for quantitative analysis. This follows in that the inclusion of Eq 2 provides an interesting property with respect to error propagation. Referring to Eq 2, one notes that the calculated temperature field, at any given time, can be "corrected" according to values of target temperatures T_n^c. It follows that by inclusion of Eq 2, which is with respect to an inverse-problem perspective, the discrete representation Eq 2 to 5 is equipped with a predictor-corrector property for calculating the time-dependent temperature field. That is to say, any error propagation that is related to timestep size, tending to cause the calculated temperature field to deviate from its correct values, is corrected for within a specified tolerance $Z_T < \varepsilon$, at those times when Eq 2 is applied. Within the context of inverse analysis, the system is assumed overdetermined to the extent that various approximations may be introduced for *further* development of the numerical method. This follows that the rigorous foundation of the method is constrained parameter optimization in the least-squares sense. Accordingly, in principle, various types of approximations are justified in that errors that are introduced will be compensated for via parameter adjustment with respect to constraint conditions based on data.

Next, the representation of the temperature field using a linear combination of numerical basis functions as defined by Eq 10 will in general be effected using numerical procedures for the determination of the weighting coefficients associated with this linear expansion. In principle, there exist many procedures for accomplishing this task, and which of these is optimal remains for further investigation. The construction of

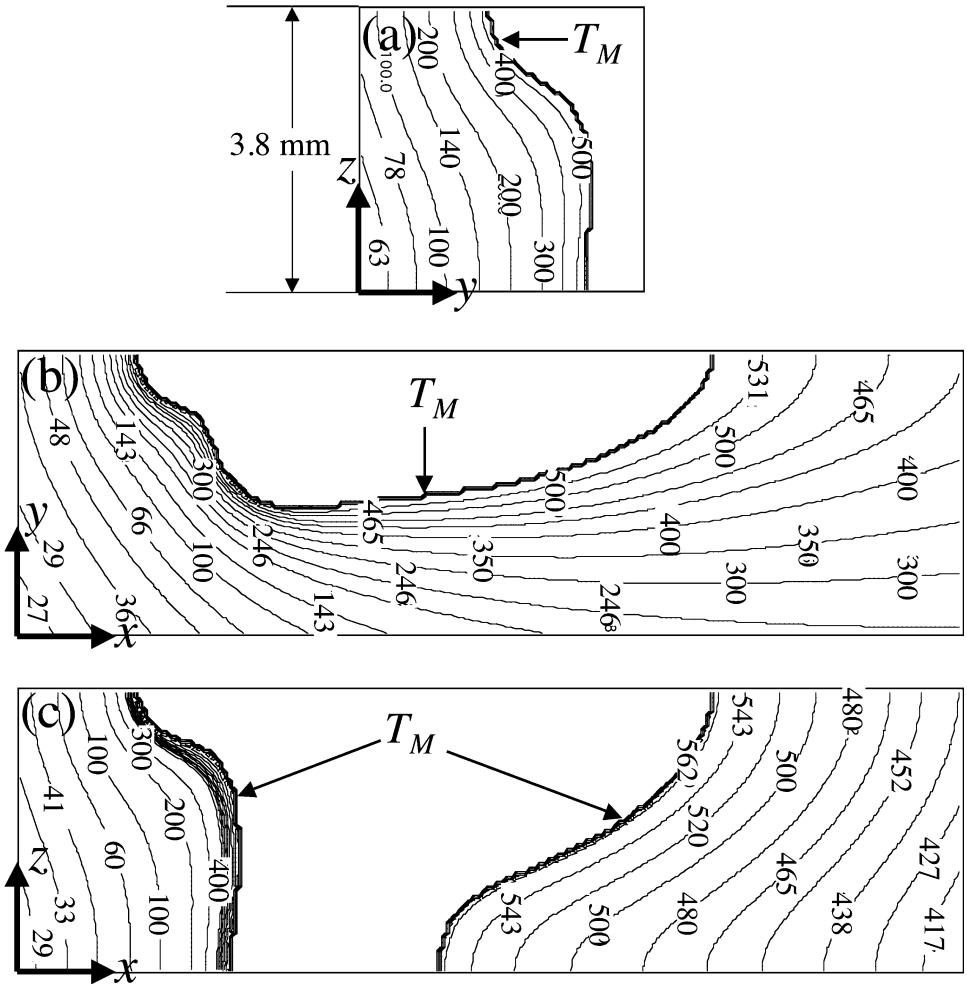

Fig. 9 Two-dimensional slices of three-dimensional temperature field (°C) calculated using cross section information shown in Fig. 6. (a) Transverse cross section. (b) Top surface of workpiece. (c) Longitudinal cross section at symmetry plane

numerical basis functions presented in the previous section represents one procedure for this task, which demonstrates both the construction and the use of numerical basis functions for calculation of temperature fields. This can be seen with reference to Table 2 to 4. First, referring to Table 2, it is to be noted that the values of the source function $C(\hat{x}_k)$ are determined by iterative adjustment until the specified constraint conditions given in Table 1 are satisfied within a reasonable tolerance according to Eq 3. This procedure represents construction of a numerical basis function. Next, it is to be noted that the values of the source function given in Table 3 and 4 are not determined according to the specified constraint conditions given in Table 1 only. The procedure for calculation of these values entails small adjustments of the coefficients A_k defined in the expression

$$T(\hat{x},t) = T_{\mathrm{A}} + \sum_{k=1}^{N_k}\sum_{n=1}^{N_t} A_k C(\hat{x}_k) G(\hat{x},\hat{x}_k,\kappa,n\Delta t), \qquad \text{(Eq 11)}$$

where the source function $C(\hat{x}_k)$ is given in Table 2. It follows, therefore, that calculation of the temperature fields shown in Fig. 9 and 10 for the welds whose cross sections are shown in Fig. 6 and 7 is in terms of linear combinations of numerical basis functions whose values are specified by Table 2.

7. Conclusion

One objective of this report is to describe a numerical method for inverse thermal analysis of steady-state energy deposition in plate structures. This method employs different types of basis functions for parametric representation of steady-state temperature fields. The specific algorithmic aspects of constructing temperature fields by means of this parameterization are for further investigation. This report represents a continuation of the attempt to make quantitative a highly qualitative experience having occurred over the course of inverse analyses applied to various types of energy deposition processes. This experience is associated with the fact that in many cases where inverse analysis was applied to a given welding process for a given set of process parameters and alloy, following procedures similar to that defined here, the temperature field having been calculated was very similar to one having been calculated previously for a significantly different welding process, set of process parameters and alloy. Accordingly, this experience establishes the existence of a multidimensional temperature field $T(\hat{x},t,\kappa,V,l,T_s(\hat{x}_s),\ \hat{x}_s \in S_{\mathrm{i}},S_{\mathrm{o}})$ for representation of welding processes in general, especially in the case of restricted geometries such as those associated with

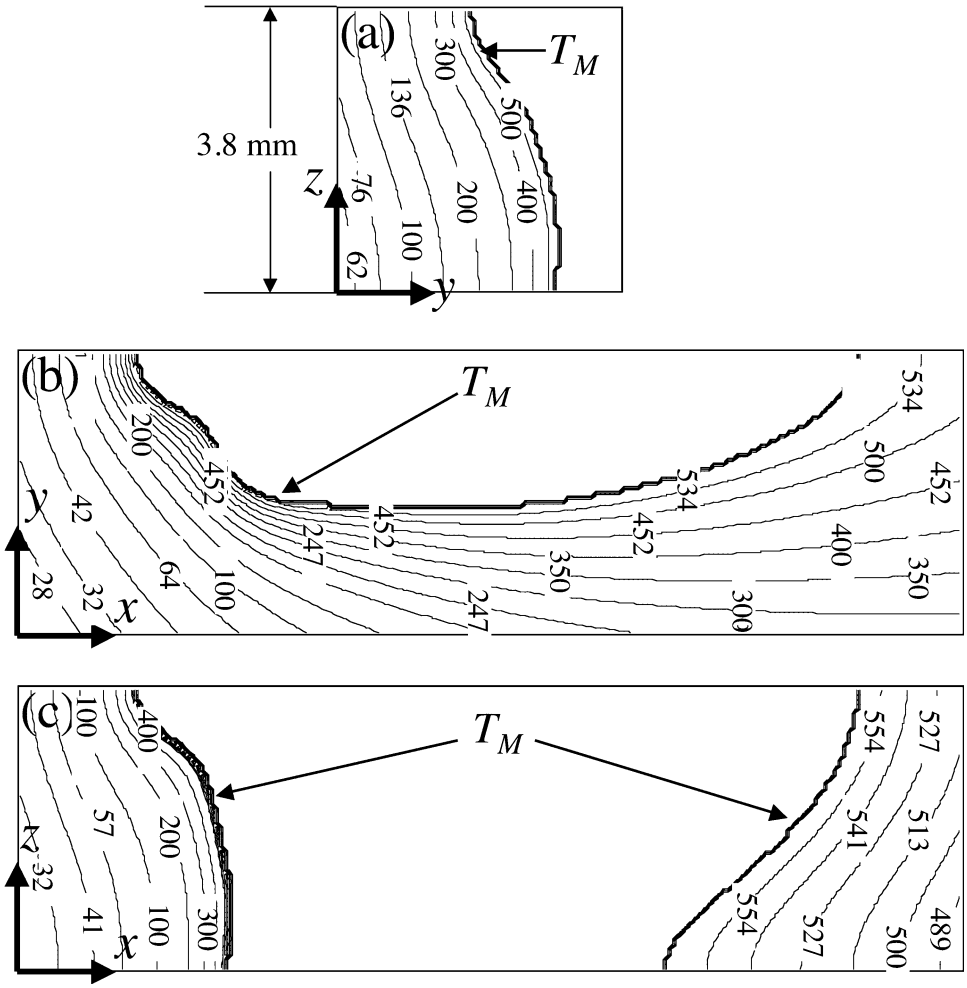

Fig. 10 Two-dimensional slices of three-dimensional temperature (°C) field calculated using cross section information shown in Fig. 7. (a) Transverse cross section. (b) Top surface of workpiece. (c) Longitudinal cross section at symmetry plane

Table 2 Volumetric source function $C(\hat{x}_k)$ calculated according to constraint conditions specified by weld cross sections shown in Fig. 5, where Δl = 3.8/60 mm

k	$C(\hat{x}_k)$/2.9	x_k (Δl)	y_k (Δl)	z_k (Δl)
1	0.042	0.0	0.0	3.0
2	0.041	0.0	0.0	5.0
3	0.038	0.0	0.0	7.0
4	0.03	0.0	0.0	9.0
5	0.03	0.0	0.0	11.0
6	0.03	0.0	0.0	13.0
k	$C(\hat{x}_k)$/1.3	x_k (Δl)	y_k (Δl)	z_k (Δl)
7	0.1	4.0	0.0	0.0
8	0.1	−4.0	0.0	0.0
9	0.1	0.0	4.0	0.0
10	0.1	0.0	−4.0	0.0

Table 3 Volumetric source function $C(\hat{x}_k)$ calculated according to constraint conditions specified by weld cross sections shown in Fig. 6, where Δl = 3.8/60 mm

k	$C(\hat{x}_k)$/2.9	x_k (Δl)	y_k (Δl)	z_k (Δl)
1	0.015	0.0	0.0	3.0
2	0.015	0.0	0.0	5.0
3	0.025	0.0	0.0	7.0
4	0.027	0.0	0.0	9.0
5	0.027	0.0	0.0	11.0
6	0.025	0.0	0.0	13.0
k	$C(\hat{x}_k)$/1.3	x_k (Δl)	y_k (Δl)	z_k (Δl)
7	0.1	4.0	0.0	0.0
8	0.1	−4.0	0.0	0.0
9	0.1	0.0	4.0	0.0
10	0.1	0.0	−4.0	0.0

plate structures. Another objective of this report was to establish rigorous conditions for the application of inverse thermal analysis using basis-function representations and associated parameterizations. Accordingly, the statement of the inverse heat deposition problem presented here provides a rigorous foundation for the validity and well posedness of the inverse analysis of welding processes, and consequently, relatively strict conditions for its application.

Table 4 Volumetric source function $C(\hat{x}_k)$ calculated according to constraint conditions specified by weld cross sections shown in Fig. 7, where Δl = 3.8/60 mm

k	$C(\hat{x}_k)$/2.9	x_k (Δl)	y_k (Δl)	z_k (Δl)
1	0.05	0.0	0.0	3.0
2	0.045	0.0	0.0	5.0
3	0.045	0.0	0.0	7.0
4	0.027	0.0	0.0	9.0
5	0.027	0.0	0.0	11.0
6	0.025	0.0	0.0	13.0
k	$C(\hat{x}_k)$/1.3	x_k (Δl)	y_k (Δl)	z_k (Δl)
7	0.1	4.0	0.0	0.0
8	0.1	−4.0	0.0	0.0
k	$C(\hat{x}_k)$/0.9	x_k (Δl)	y_k (Δl)	z_k (Δl)
9	0.1	0.0	4.0	0.0
10	0.1	0.0	−4.0	0.0

Acknowledgments

One of the authors (SGL) acknowledges the support by the Naval Research Laboratory (NRL) internal core program and active scientific collaboration with the University of Thessaly. The authors (ADZ, GNH) would like to thank the German Research Foundation DFG for the support of the depicted research within the Cluster of Excellence "Integrative Production Technology for High-Wage Countries" at RWTH Aachen University." Also ADZ acknowledges the support of Dr. Alexander Drenker of Fraunhofer-Institut für Lasertechnik during experimental work.

References

1. S.G. Lambrakos, A.D. Zervaki, G.N. Haidemenopoulos, and V. Stergiou, *Basis Functions and Parameterizations for Inverse Analysis of Welding Processes, Mathematical Modelling of Weld Phenomena*, Vol 9, Verlag der Technischen Universite, Graz, 2011, p 793–815
2. A.D. Zervaki, G.N. Haidemenopoulos, and S.G. Lambrakos, *Analysis of Heat Affected Zone using Direct and Inverse Modelling in 6XXX Aluminum Alloys, Mathematical Modelling of Weld Phenomena*, Vol 8, Verlag der Technischen Universite, Graz, 2007, p 907–923
3. S.G. Lambrakos and S.G. Michopoulos, *Algorithms for Inverse Analysis of Heat Deposition Processes, Mathematical Modelling of Weld Phenomena*, Vol 8, Verlag der Technischen Universite, Graz, 2007, p 847–879
4. S.G. Lambrakos and J.O. Milewski, *Analysis of Welding, Heat Deposition Processes Using an Inverse-Problem Approach, Mathematical Modelling of Weld Phenomena*, Verlag der Technischen Universite, Graz, 2005, p 1025–1055
5. J. Xie and J. Zou, Numerical Reconstruction of Heat Fluxes, *SIAM J. Numer. Anal.*, 2005, **43**(4), p 1504–1535
6. A. Tarantola, *Inverse Problem Theory and Methods for Model Parameter Estimation*, SIAM, Philadelphia, PA, 2005
7. H.S. Carslaw and J.C. Jaegar, *Conduction of Heat in Solids*, Vol 374, 2nd ed., Clarendon Press, Oxford, 1959
8. S.V. Patankar, *Numerical Heat Transfer and Fluid Flow*, Hemisphere Publishing, New York, 1980